Egypt. J. Geo. **Vol. 67,** pp: 123-134 (2023)

Egyptian Journal of Geology

https://egjg.journals.ekb.eg

Source rock evaluation of Jurassic rock units for Imhotep field, Matruh basin, Western Desert, Egypt

El-Shorbagy, A.I.[1]*; Doaa A. Mousa[2] and **Mahmoud Y. Zein El Din[1].**

[1] *Al- Azhar University- Faculty of Science-Geology Department. Cairo, Egypt*
[2] *Egyptian Petroleum Research Institute [EPRI]. Cairo, Egypt*

More advanced techniques in organic geochemical evaluation and geoscience integration reveal clear understanding of oil field stories. The Imhotep field represents one of these wild oil fields in Western Desert. This study may represent the first comprehensive work to evaluate this field. Selected eighty-four (84) ditch samples and "4" extract samples representing Lower Safa and Upper Safa members were gathered from five wells (Imhotep-1X, Imhotep-2X, Imhotep W-1X, Imhotep S-1X, and Imhotep S-3X) to conduct this study. The samples were examined utilizing LECO C230, Rock–Eval-6 and GC techniques. The studied sample analysis demonstrates that the Total Organic Carbon content (TOC) extends from poor to excellent hydrocarbon potentiality. The maturity evaluation using Tmax and the calculated Vitrinite reflectance (Ro) revealed that the extracted samples have good thermal maturation and attain the oil generation stage. Also, the analysis revealed that the kerogen of study samples is mixed type II/III kerogen, and this reflects the potential to generate gas and oil and reach the final phase of oil generation. The GC results suggest that the organic matter is marine, mixed with terrestrial input, and the deposition was under reducing to a suboxic environment.

Keywords: Biomarker; GC analysis; Geochemical analysis; Jurassic Rocks; Kerogen type; Matruh Basin; Rock Eval-6.

1. Introduction

The Western Desert in Egypt covered about 700.000 square kilometers and comprises more than two-thirds of the whole area of Egypt. In Western Desert the sedimentary section ranges from lower Paleozoic to Recent. Many crucial gas and oil fields were specifically discovered in its Northern part.

The area under study (Imhotep field) (**Figure 1**) is in Matruh basin. One of northern Egypt's conventional hydrocarbons producing basins is the Matruh Basin. The production and exploration activities in Matruh Basin focused on the Cretaceous and Jurassic rocks (Deaf, 2021). Quite recent times, gratitude to modern technologies and innovative methodologies of exploration (e.g., El-Sharkawy, 2018; Dolson, 2020), promising hydrocarbon potential was documented from some Paleozoic rocks. This shows some need to carry out comprehensive studies to explore the prospective of the Matruh Basin more effectively. Little attention has been given by some authors to the middle upper Jurassic strata represented by the Khatatba (Lower and Upper Safa members) and Masajid formations (e.g., Al-Sharhan et al., 2008; Shalaby et al., 2011; Felestteen et al., 2014; El Diasty, 2015; Abdel-Gawad et al., 2015). Middle Jurassic Khatatba Formation strata were deposited in broad fluvial flood plains with overbank swamps and small lakes transitional to estuarine or lagoonal environments (Bosworth, William. 2015). The crude oil geochemical data in Matruh Basin support a complex charge history from a single source rock, rather than mixing of oils from two source rocks (Michael A. Abrams. et al., 2016).

The study area lies between latitudes 30o 50` 35`` – 30o 54` 38`` N and longitudes 27o 20` 46`` - 27o 25` 16``E.

The stratigraphic section of the northwestern Desert includes a sedimentary section ranging in age from the basement that occurs in Pre-Cambrian to the

*Corresponding author e-mail: ali.ismail@azhar.edu.eg
Received: 20/03/2023; Accepted: 24/06/2023
DOI: 10.21608/EGJG.2023.200603.1041

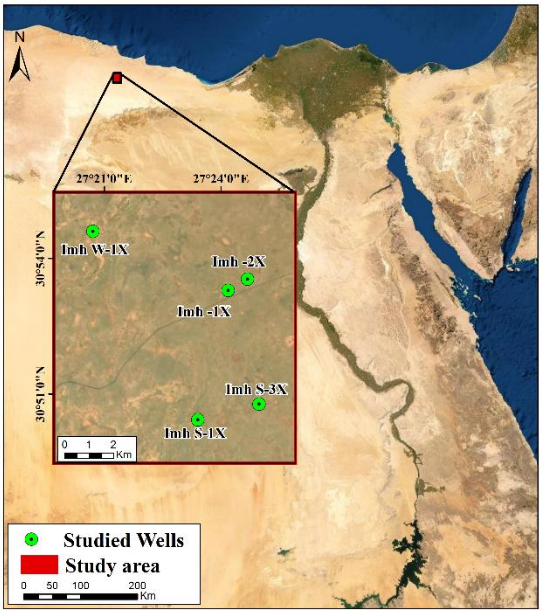

Fig. 1. Location map of the study area.

Recent formations (**Figure 2**). The far Western Desert basins record a complex geologic past that spans from the Neoproterozoic to the Recent (Abdelbaset, m. et al. 2022). The Khatatba formation of the area under study represented in all the studied wells is subdivided into three members: 1. Lower Safa Member, 2. Upper Safa Member and 3. Zahra Member (**Figure 2**) and consists mainly of sandstone and shale with siltstone and limestone streaks. We could not get samples for Zahra Member to analyze (**Figure 2**).

The primary goal of this investigation is to evaluate the source of the Imhotep field, and this can be reached by: (i) determining and describing potential source rocks and their generating capability (ii) to investigating the maturation levels of the expected source of oil preservation, and (iii) to predict the environment of deposition for the preserved organic matter.

2. Materials and Methods

Eighty-four (84) cutting samples consist mainly of Limestone and argillaceous shales representing Jurassic rock unit (Lower Safa and Upper Safa members) from wells (Imhotep-1X, Imhotep-2X, Imhotep W-1X, Imhotep S-1X, and Imhotep S-3X) in Imhotep field were analysed.

2.1 Pyrolysis analysis 2.1.1

The samples have been analyzed by LECO C230 to measure the Total Organic Carbon (TOC, wt %), and Rock-Eval 6 was employed for pyrolysis analysis. Four (4) extract samples representing Lower Safa and Upper Safa members. Below is a quick explanation of the techniques that were used:-

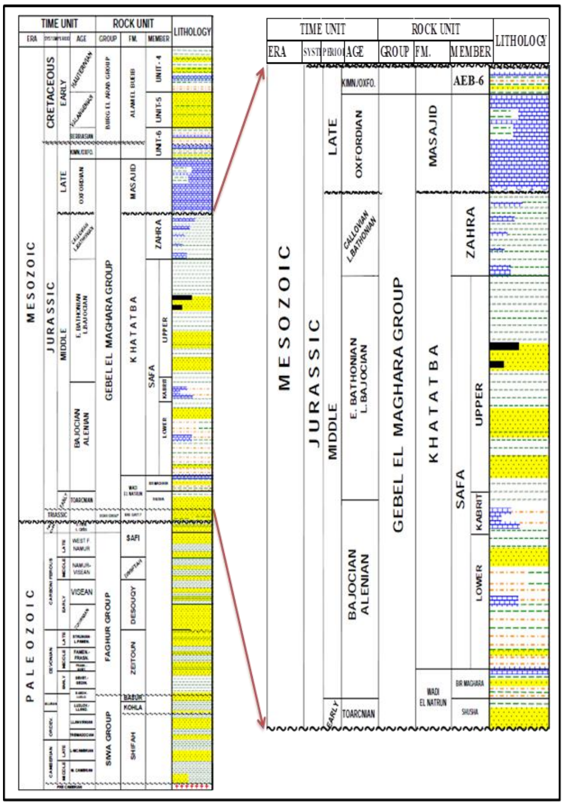

Fig. 2. A Generalized stratigraphic column of the Northwestern Desert (Khalda, 2001).

Clean-up was accomplished on the samples, crushed, and screened through 200 mesh for total organic carbon and Rock-Eval pyrolysis using established procedures. The selected samples were subjected to geochemical analysis. About 0.140-0.150 grams of sample was placed in a crucible with 5% HCl at 80.°C to remove carbonates. Using a LECO C230 instrument, total organic carbon content (TOC) was determined. The LECO C230 uses an induction furnace and measures carbon by infrared absorption.

2.1.2 Rock-Eval pyrolysis was performed on pulverized whole rock samples (~60 mg) using a Vinci Rock-Eval 6 pyro-analyzer in the bulk rock mode. This method was used to produce free hydrocarbons S_1(mg.HC/g.rock), and residual petroleum potential S_2 (mg.HC/g.rock), S_3 (CO_2 derived from kerogen pyrolysis). All these factors are used in the present work to calculate the Hydrogen Index (HI.mg.HC/g.TOC) and Oxygen Index (OImgCO_2/gTOC).

2.2. Gas Chromatography (GC) analysis

Concerning the screening results, preferred samples are utilized for extraction using Soxhlet apparatus to separate bitumen from rock samples with organic solvent (Chloroform). Bitumen is extracted by pulverizing the rock (~10 gm) and then soaking the pulverizing rock for 12 to 36 hr in an organic solvent (chloroform). The solvent is removed from bitumen by evaporation (this method of removal results in the absence of the lighter hydrocarbons, which have a similar evaporation rate as the solvent). In practice, only hydrocarbons heavier than carbon number C_{15}+ are retained for further analysis. The extracted bitumen is expressed as weight percent to the whole rock sample. Removal of elementary sulfur from extracted bitumen by mercury. Asphaltene was separated from the extracted bitumen using n-hexane. The saturated fractions of rock extracts samples were analyzed with Hewlett Packard (HP) 6890 Series GC System/ Agilent 6890 Series Injector. A capillary column is used to provide separation of the hydrocarbon compounds in the n-C_4 to n-C_{42} carbon range for detection by Flame Ionized Detector (FID). These examinations had been carried out in laboratories of the StratoChem Services Lab. (SCS).

3. Results 3.1. Source Rock Evaluation

Rock-Eval pyrolysis results and TOC for "41" ditch samples represent Lower Safa Member and “43” ditch samples representing Upper Safa Member from wells (Imhotep-1X, Imhotep-2X, Imhotep W-1X, Imhotep S-1X, and Imhotep S-3X) were analyzed based on geochemical methods e.g., TOC/Rock-Eval pyrolysis and molecular analysis. The pyrolysis results are represented in **Tables 1 and 2**.

3.1.1. Organic Richness and Hydrocarbon Potentiality

The measured organic content of the present samples of Lower Safa Member, displays a large variety of variance in TOC content which ranges from 0.44 to 10.5 wt% (**Table 1**). The TOC and depth relation diagram (**Figure 3**) shows that Lower Safa Member is extended from poor through excellent source rock. Upper Safa Member TOC ranges from 0.77 to 9.98 wt % (**Table 2**) stating that the organic matter abundance varies from fair to excellent source rock (**Figure 3**). owever, TOC used with caution independently for several reasons, along with inert organic carbon (Tissot et al., 1974), thermal maturity (Daly and Edman., 1987) and oil contamination (Carvajal-Ortiz and Gentzis 2015), could influence this parameter. Based on TOC and S_2 plot (**Figure 4**), most samples that were examined of Lower Safa Member shows poor to excellent source (**Table 1 and Figure 4**) while Upper Safa Member indicate fair to excellent source rock (**Table 2 and Figure 4**). Considering the diagram, the wide variety of the representative members may reflect variable depositional conditions or subsequent regression and transgression of sea level throughout deposition

3.1.2. Kerogen type

Pyrolysis parameters like S_2 (kerogen yield), Hydrogen Index. (HI), and Oxygen Index. (OI) are extremely helpful for supplying information about kerogen types for the present samples. On the TOC versus S_2 diagram (**Figure 5**) the sampling distribution of Lower Safa Member are between type III and type II/III kerogen. The Hydrogen Index of Lower Safa Member ranges from 36 to 147 (mg/g) and Oxygen Index (OI) ranges from 19 to 460 (mg/g) (**Table 1**) suggesting kerogen type II/III as depicted in the modified Van Krevelen diagram (**Figure 6**). Upper Safa Member has (HI) ranges 46 to 138 mg/g and Oxygen Index from 18 to 368 mg/g (**Table 2**) suggesting kerogen type II/III (**Figure 6**), the figure TOC vs. HI (**Figure 7**) confirms the mentioned data (**Figure 7**) as it depicts the main produced hydrocarbon is oil/gas with fair oil source. It is significant to consider that the oxygen index values suggest less anoxic environment of deposition, therefore less oxidation and good preservation for organic matter through deposition (Shekarifard et al. 2019). Moreover, it should not be dismissed that (OI) values may be influenced by the type of precursor organic matter in the maturation stage.

3.1.3. Thermal Maturation of Organic Matter

Thermal transformation of organic matter performs significant participation in hydrocarbon generation. Rock-Eval pyrolysis is a common maturation parameter. The thermal maturation levels for the studied source rock samples have been established with ‘‘Tmax” representing temperature (℃) where the S_2 peak is its maximum value., Tmax value from the rock eval as maturity indicator must be used with caution as it is influenced by the mineral matrix, and type of organic matter, and has a good relationship with Ro, production index ‘‘PI” and the pyrolysis hydrogen index (HI). The pyrolysis Hydrogen Index vs. ‘‘Tmax” (**Figure 8**) indicates mature source rocks and kerogen type III with mixed type II/III in Lower Safa and Upper Safa members (**Figure 8**). Tmax values of the study samples vary from 442 to 484 ^{o}C (**Tables 1 and 2**) had shown that most samples are mature. This is agreeing with the plot of the production index (PI) with Tmax which indicates mature to late stage of maturation source rocks (**Figure 9**). Vitrinite

Table 1. Pyrolysis data for Lower Safa Member.

Well	Depth	TOC	S_1	S_2	S_3	Tmax	HI	OI	PI	S_1+S_2	Calc. Ro
	15180	0.93	0.05	0.81	1.07	464	87	115	0.06	0.86	1.19
	15280	0.57	0.09	0.42	2.27	463	74	401	0.18	0.51	1.17
	15400	1.01	0.05	0.84	3.09	465	83	306	0.06	0.89	1.21
Imhotep-1X	15480	0.69	0.04	0.65	1.79	465	95	261	0.06	0.69	1.21
	15550	1.34	0.06	0.94	3	463	70	224	0.06	1	1.17
	15760	0.58	0.07	0.28	2.51	464	48	430	0.2	0.35	1.19
	15810	0.82	0.05	0.34	1.06	460	42	130	0.13	0.39	1.12
	15830	3.99	0.08	4.96	2.1	459	124	53	0.02	5.04	1.10
	15900	0.89	0.04	0.56	1.61	458	63	182	0.07	0.6	1.08
	15960	0.61	0.04	0.23	1.18	460	38	194	0.15	0.27	1.12
Imhotep-2X	15150	0.59	0.06	0.39	2.09	473	66	356	0.13	0.45	1.35
	15300	2.18	0.1	1.56	1.64	478	72	75	0.06	1.66	1.44
	15310	0.48	0.04	0.29	1.86	472	60	388	0.12	0.33	1.34
	15350	0.88	0.06	0.45	2.81	471	51	319	0.12	0.51	1.32
	15410	0.44	0.05	0.24	2.01	468	55	460	0.17	0.29	1.26
	15460	0.85	0.06	0.3	2.84	471	36	336	0.17	0.36	1.32
	15550	0.77	0.06	0.32	2.57	472	41	332	0.16	0.38	1.34
Imhotep W-1X	14680	1.26	0.12	1.12	4.64	463	89	368	0.10	1.24	1.17
	14790	2.77	0.11	2.43	2.42	466	88	87	0.04	2.54	1.23
	14920	1.54	0.12	0.86	3.72	468	56	242	0.12	0.98	1.26
	15020	1.73	0.1	1.11	3.59	455	64	208	0.08	1.21	1.03
	13740	4.12	0.3	5.15	1.34	455	125	33	0.06	5.45	1.03
	13770	1.02	0.27	1.08	1.77	446	106	174	0.2	1.35	0.87
	13930	2.02	0.24	1.82	2.37	456	90	117	0.12	2.06	1.05
Imhotep S-1X	14000	1.83	0.28	2.02	1.83	456	110	100	0.12	2.3	1.05
	14120	2.12	0.25	2.28	2.77	457	108	131	0.1	2.53	1.07
	14250	2.51	0.28	2.67	2.43	454	106	97	0.09	2.95	1.01
	14330	5.67	0.34	6.71	1.71	459	118	30	0.05	7.05	1.10
	13850	1.95	0.17	1.29	2.15	458	66	110	0.12	1.46	1.08
	13940	0.87	0.18	0.63	3.07	442	72	352	0.22	0.81	0.80
	13990	2.13	0.22	2	2.33	460	94	109	0.1	2.22	1.12
	14050	9.01	0.3	10	1.65	464	111	18	0.03	10.3	1.19
Imhotep S-3X	14110	3.73	0.19	3.93	1.19	467	105	32	0.05	4.12	1.25
	14280	1.29	0.17	0.84	2.45	461	65	190	0.17	1.01	1.14
	14350	1.1	0.14	0.6	1.43	474	55	130	0.19	0.74	1.37
	14400	1.49	0.17	0.78	1.71	458	52	115	0.18	0.95	1.08
	14470	0.81	0.14	0.41	1.66	444	50	204	0.25	0.55	0.83
	14570	1.44	0.19	0.66	1.81	473	46	126	0.22	0.85	1.35

N.B.
TOC : Total organic carbon(weight percent of the whole rock).
S_1 : Free hydrocarbon (mg hydrocarbon/g rock).
S_2 : Hydrocarbon potentiality (mg hydrocarbon/g rock).
HI : Hydrogen index (mg hydrocarbon/g TOC).
OI : Oxygen index (mg CO2/g TOC).
Tmax : Temperature at which maximum emission of high temperature (S_2) hydrocarbon occurs (deg.oC.).
PI : Production index (S_1/S_1+S_2).
(Calculcated %VRo) = (0.0180) (Tmax)- 7.16.

Table 2. Pyrolysis data for Upper Safa Member.

Well	Depth	TOC	S_1	S_2	S_3	Tmax	HI	OI	PI	S_1+S_2	Calc. Ro
	14550	2.62	0.08	2.01	3.19	458	77	122	0.04	2.09	1.08
	14600	0.89	0.07	0.7	1.87	454	78	210	0.09	0.77	1.01
	14650	9.95	0.19	14.15	3.37	465	100	24	0.01	14.34	1.21
Imhotep-1X	14730	7.7	0.13	8.59	2.05	463	112	27	0.01	8.72	1.17
	14760	0.77	0.05	0.58	1.49	458	76	195	0.08	0.63	1.08
	14780	2.91	0.08	2.96	0.9	463	102	31	0.03	3.04	1.17
	14930	2.93	0.09	4.04	5.39	460	138	184	0.02	4.13	1.12
	15060	4.03	0.07	3.33	2.92	453	83	72	0.02	3.4	0.99
	14460	2.67	0.08	2.15	3.64	462	81	136	0.04	2.23	1.16
	14550	2.51	0.11	2.04	6.04	463	81	241	0.05	2.15	1.17
	14590	9.79	0.18	10.6	3.35	460	108	34	0.02	10.78	1.12
	14630	1.62	0.07	1.23	2.63	454	76	162	0.05	1.3	1.01
Imhotep-2X	14790	0.88	0.07	0.78	2.49	470	89	283	0.08	0.85	1.30
	14850	1.47	0.09	0.91	5.14	468	62	350	0.09	1	1.26
	14890	1.14	0.09	0.82	4.15	470	72	364	0.1	0.91	1.30
	14900	9.98	0.21	12.54	2.4	463	116	22	0.02	12.75	1.17
	14920	2.5	0.09	1.58	2.16	467	63	86	0.05	1.67	1.25
	15020	2.08	0.08	1.34	2.7	471	64	130	0.06	1.42	1.32
	14350	4.19	0.1	3.99	2.66	460	95	63	0.02	4.09	1.12
	14380	1.79	0.09	1.4	3.44	456	78	192	0.06	1.49	1.05
Imhotep W-1X	14430	2.13	0.10	1.41	3.74	455	66	176	0.07	1.51	1.03
	14560	0.9	0.07	0.83	2.6	454	92	289	0.08	0.9	1.01
	14680	1.26	0.12	1.12	4.64	463	89	368	0.10	1.24	1.17
	14790	2.77	0.11	2.43	2.42	466	88	87	0.04	2.54	1.23
Imhotep W-1X	14920	1.54	0.12	0.86	3.72	468	56	242	0.12	0.98	1.26
	15020	1.73	0.1	1.11	3.59	455	64	208	0.08	1.21	1.03
	13740	4.12	0.3	5.15	1.34	455	125	33	0.06	5.45	1.03
	13770	1.02	0.27	1.08	1.77	446	106	174	0.2	1.35	0.87
	13930	2.02	0.24	1.82	2.37	456	90	117	0.12	2.06	1.05
Imhotep S-1X	14000	1.83	0.28	2.02	1.83	456	110	100	0.12	2.3	1.05
	14120	2.12	0.25	2.28	2.77	457	108	131	0.1	2.53	1.07
	14250	2.51	0.28	2.67	2.43	454	106	97	0.09	2.95	1.01
	14330	5.67	0.34	6.71	1.71	459	118	30	0.05	7.05	1.10
	13850	1.95	0.17	1.29	2.15	458	66	110	0.12	1.46	1.08
	13940	0.87	0.18	0.63	3.07	442	72	352	0.22	0.81	0.80
	13990	2.13	0.22	2	2.33	460	94	109	0.1	2.22	1.12
	14050	9.01	0.3	10	1.65	464	111	18	0.03	10.3	1.19
	14110	3.73	0.19	3.93	1.19	467	105	32	0.05	4.12	1.25
Imhotep S-3X	14280	1.29	0.17	0.84	2.45	461	65	190	0.17	1.01	1.14
	14350	1.1	0.14	0.6	1.43	474	55	130	0.19	0.74	1.37
	14400	1.49	0.17	0.78	1.71	458	52	115	0.18	0.95	1.08
	14470	0.81	0.14	0.41	1.66	444	50	204	0.25	0.55	0.83
	14570	1.44	0.19	0.66	1.81	473	46	126	0.22	0.85	1.35

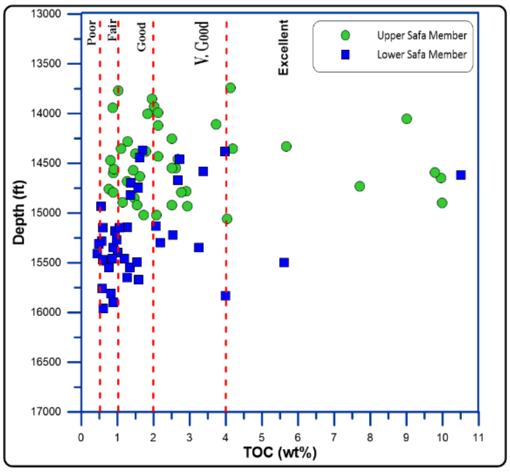

Fig. 3. Cross plot of TOC versus depth of Lower and Upper Safa members in the studied wells, Imhotep field, Western Desert, Egypt (Peters and Cassa, 1994).

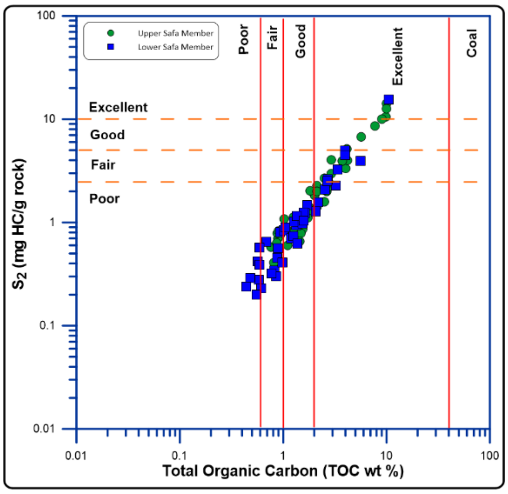

Fig. 4. Organic richness and hydrocarbon potentialities of the studied samples, Imhotep field, Western Desert, Egypt

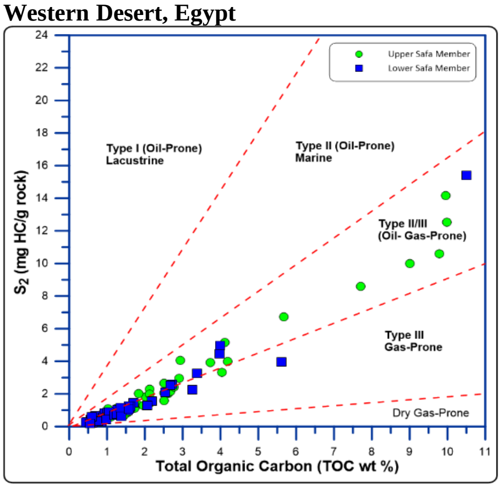

Fig. 5. TOC versus S_2 cross plot for the analyzed samples from the Lower and Upper Safa members in the studied wells, Imhotep field (Dahl et al., 2004)

reflectance (Ro) is a maturity indicator based on the characteristics of a single type of organic particle.

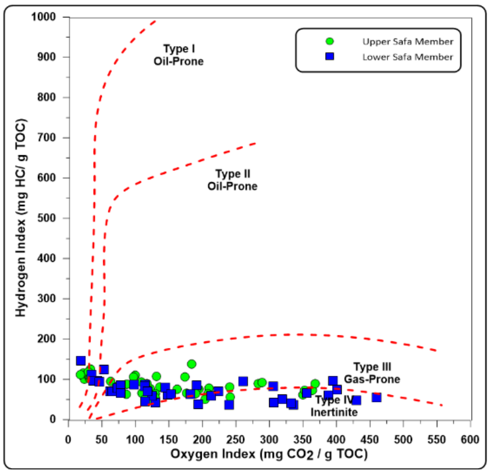

Fig. 6. Modified Van Krevelen Diagram Showing Kerogen Type of the studied samples (Espitalie et al., 1977).

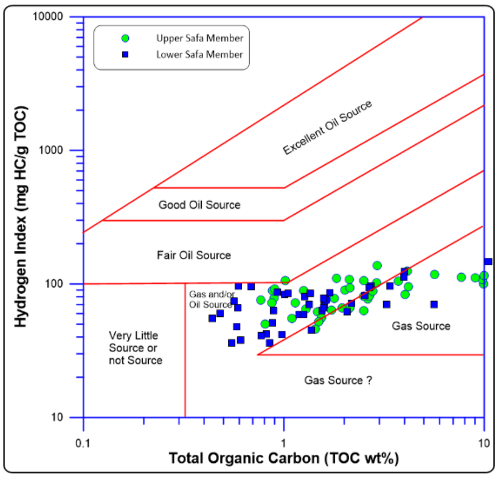

Fig. 7. Source rock characterization using plot of HI versus TOC for the studied samples (Jackson et al., 1985)

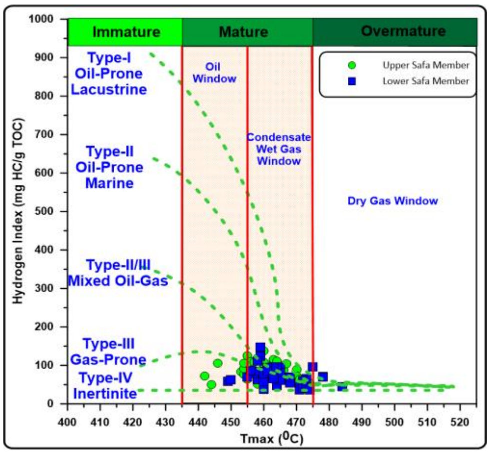

Fig. 8. Cross plot of hydrogen index (HI) versus Tmax of the studied samples, Imhotep field, Western Desert, Egypt (Espitalie et al., 1985).

Calculated Vitrinite reflectance (Ro) of Lower and Upper Safa members values ranging between 0.80

and 1.55 % matches with the previous maturation parameters and occurs in the plot of calculated Vitrinite reflectance (Ro) with hydrogen index (HI) (Hunt, 1996) (**Figure 10**).

3.2. Source Rock Evaluation using Biomarkers.

3.2.1. Normal Alkanes

The fingerprint of gas chromatography of the Lower Safa Member represented by 2 extracted samples from wells (Imhotep-1X and Imhotep S-1X) (**Figure 11 a** and **b**) and the calculated parameters in **Table (3)**, showing that Lower Safa Member contains kerogen type II/III with maximum concentration peak of normal alkanes from C_9 to C_{37} with remarkable C_{17} peak, indicating input of terrestrial organic matter with aquatic organic input. Also, the Lower Safa Member is characterized by CPI values equal to 0.97 and 1.00 (**Table 3**), which suggests that its origin may be a marine organic source (Mixed type II/III Kerogen reaching the stage of maturation). The fingerprint of gas chromatography of the Upper Safa Member is represented by 2 extracted samples (**Figure 11 c and d**), from wells (Imhotep W-1X and Imhotep S-3X). These figures revealed that the Upper Safa Member contains type II/III kerogen which is distinguished by the maximum concentration peak of normal alkanes from C_{15} to C_{25} indicating a significant input of marine organisms with contribution of terrestrial organic remains. Also, the Upper Safa Member is distinguished by CPI values equal to 0.95 and 1.01 in **Table (3)**, indicating the predominance of marine organic matter (Mixed type II/III kerogen) deposited under slightly oxidizing conditions.

3.2.2. Pristane / Phytane ratio

Pristane (Pr) and Phytane (Ph) are remarkable for the evaluation of the source rock (Powell and Mckirdy. 1973). Pr/Ph ratios higher than 3 indicate an oxic depositional environment, from 1 to 3 indicate a suboxic environment of deposition, finally less than one indicates an anoxic environment of deposition (Philp 1985; Collister et.al. 2004). In Lower Safa Member, the Pr/Ph ratios range from 0.50 to 0.84 (**Table 3**) and the isoprenoids/n-alkanes (Pr/n-C_{17}) is < 0.5 which indicates mainly marine organic matter under an anoxic environment of deposition. The plot CPI versus Pr/Ph confirmed the same conclusion area under reducing conditions (**Figure 12**). According to Williams et al. (1995) Pr/Ph ratio of the Upper Safa Member shows marine and/or lacustrine shale deposits (**Table 3**) with aerobic bacterial activity according to Lijmbach (1975) and mixed depositional environment (Abdullah et.al. 1999), the isoprenoids/n-alkanes (Pr/n-C_{17}) is <0.5 reflecting that it was deposited under reducing to slightly oxidizing or suboxic environment (**Table 3**). CPI versus Pr/Ph relationship confirmed the same conclusion that the area was under reducing to slightly oxidizing or suboxic condition (**Figure 12**). Relationship between Pr/n-C_{17} versus Ph/n-C_{18} of Lower Safa Member shows a sample from well Imhotep-1X with marine organic matter input (**Figure 13**) confirmed as type I kerogen (**Figure 14**), while a sample from Imhotep S-1X has mixed organic matter (**Figure 13**) confirmed as type II/III kerogen (**Figure 14**). The Pr / Ph ratio of the Upper Safa Member is unity and ranges from 1.07 to 1.6 (**Table 3**) suggesting oxidizing environment with less restricted conditions (Didyk et al. 1978).

The plot of Pr/n-C_{17} versus Ph/n-C_{18} indicates that the Upper Safa Member is characterized by mixed organic matter under reducing to the slightly oxidizing or suboxic environment (**Figure 13**), also these ratios suggest kerogen type II and or Type II/III organic matter (**Figure 14**).

4. Conclusion

The analysis reveals that the TOC content for Lower Safa and Upper Safa members ranges from poor to excellent, with fair to excellent hydrocarbon potentiality. The maturity evaluation using Tmax, and calculated Ro revealed that the samples have very high Tmax values reflecting over mature samples reaching the gas generation stage. In addition, the results showed that the type of kerogen is a mixture of type III kerogen with a contribution of type II/III kerogen, this result reflects a potential generation of gas and oil. The GC results indicate

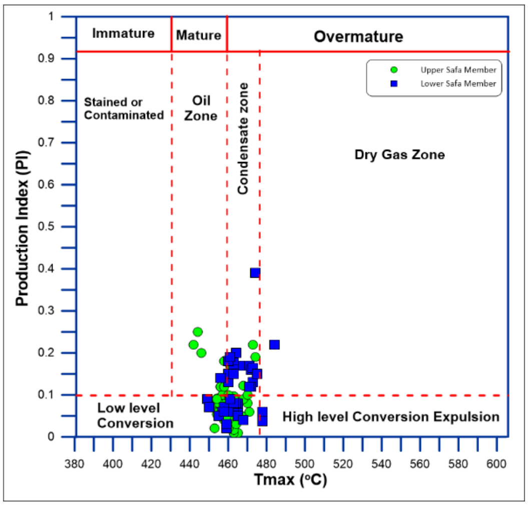

Fig. 9. Cross plot of Tmax versus PI of the studied samples, Imhotep field, Western Desert, Egypt (modified from Langford and Blank-Valleron, 1990).

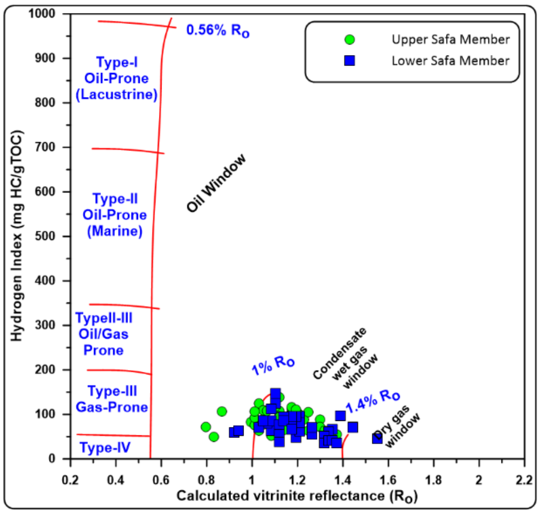

Fig. 10. HI versus calculated Ro of Lower and Upper Safa members in the studied wells, Imhotep field, Western Desert, Egypt (Hunt., 1996).

that the organic matter of Lower Safa Member is mainly marine deposited under reducing conditions, whereas the Upper Safa Member reflects marine source rock with little contribution of terrestrial organic matter deposited in shale dominant environment under high anoxic conditions than that of Lower Safa Member with a contribution for higher plants input.

Ethics approval and consent to participate: This article does not contain any studies with human participants or animals performed by any of the authors.

Consent for publication: All authors declare their consent for publication.

Funding: authors did not receive any fund from any organization

Conflicts of Interest: The author declares no conflict of interest.

Contribution of Authors: All authors shared in writing, editing and revising the MS and agree to its publication.

Acknowledgements

The authors are very grateful to the Egyptian General Petroleum Corporation (EGPC) and Khalda Petroleum Company (KPC) for providing samples and well logs of this work. Special thanks also go to Stratochem Services Company (SCS) for performing all analyses. The authors appreciate the time and efforts of the reviewers.

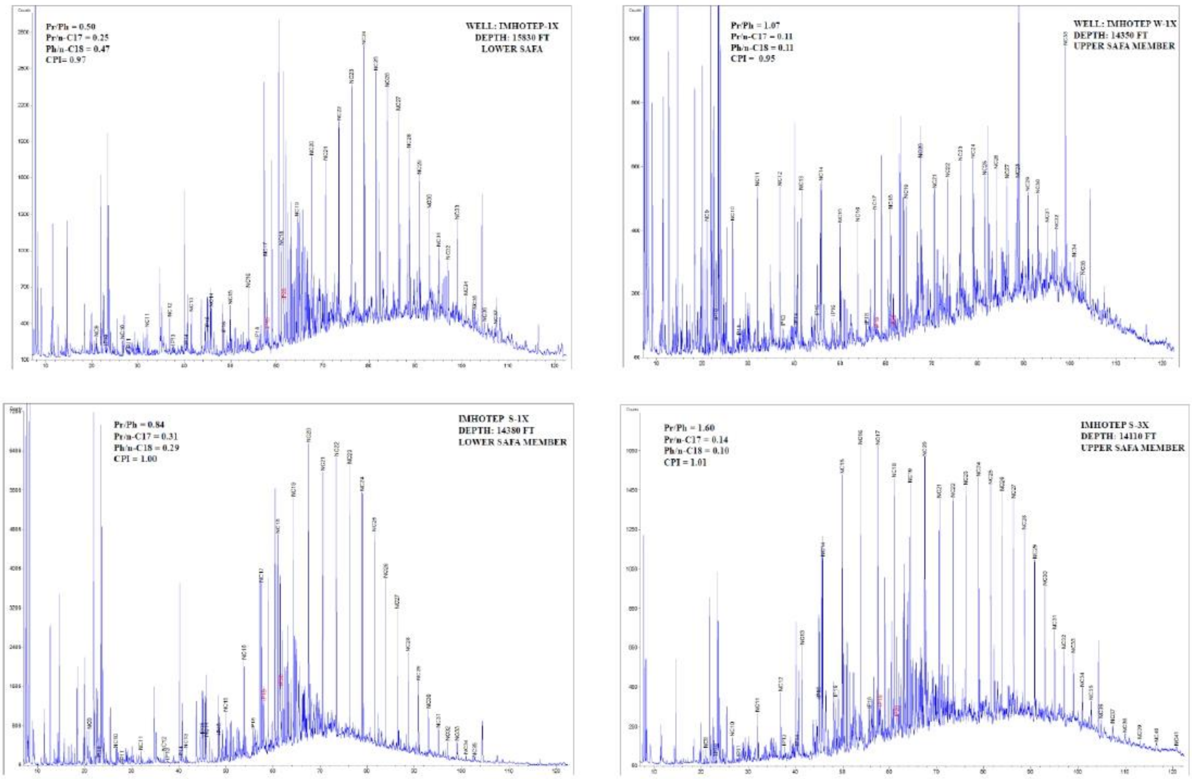

Fig. 11. Gas chromatograms for samples from Imhotep field.

Table 3. Gas chromatography results of extracted samples from Lower and Upper Safa members, Imhotep field, Western Desert, Egypt.

Formation	Well	Depth (ft)	Pr/Ph	$Pr/n\text{-}C_{17}$	$Ph/n\text{-}C_{18}$	CPI
Lower Safa Member (Extract sample)	Imhotep -1X	15830	0.50	0.25	0.47	0.97
	Imhotep S-1X	14380	0.84	0.31	0.29	1.00
Upper Safa Member (Extract sample)	Imhotep W-1X	14350	1.07	0.11	0.11	0.95
	Imhotep S-3X	14110	1.60	0.14	0.10	1.01

N.B

Pr/Ph: Isoprenoid C_{19} (Pristane)/ Isoprenoid C_{20} (Phytane)

$Pr/n\text{-}C_{17}$: Isoprenoid C_{19} (Pristane)/ Normal Alkane C_{17}

$Ph/n\text{-}C_{18}$: Isoprenoid C_{20} (Phytane)/ Normal Alkane C_{18}

CPI: ((Normal Alkane C_{23}+ Normal Alkane C_{25}+ Normal Alkane C_{27})+(Normal Alkane C_{25}+ Normal Alkane C_{27}+ Normal Alkane C_{29}))/(2*(Normal Alkane C_{24}+ Normal Alkane C_{26}+ Normal Alkane C_{28}))

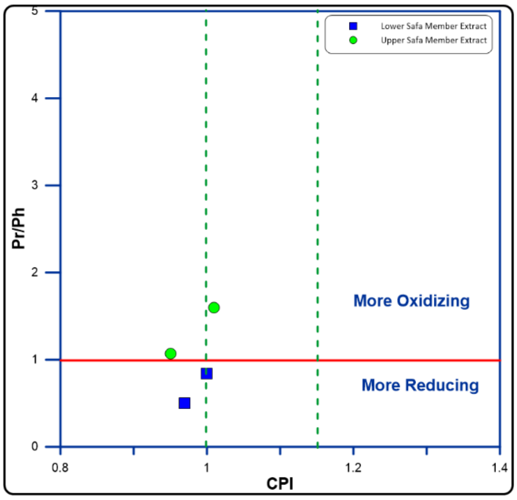

Fig. 12. Cross plot of Pr/Ph versus CPI (after Akinlua, 2007).

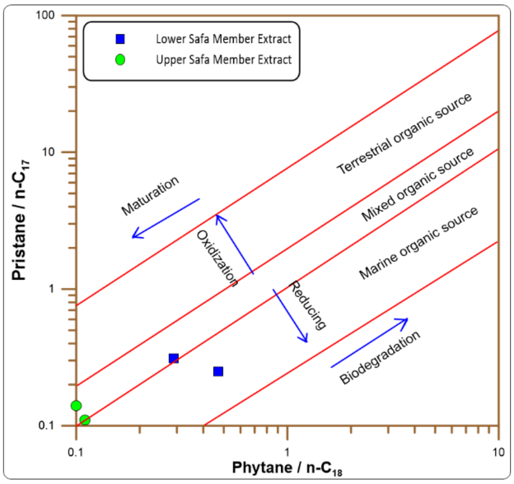

Fig. 13. Pr/n-C_{17} versus Ph/n-C_{18} cross plot, (modified after Peters et al., 1999).

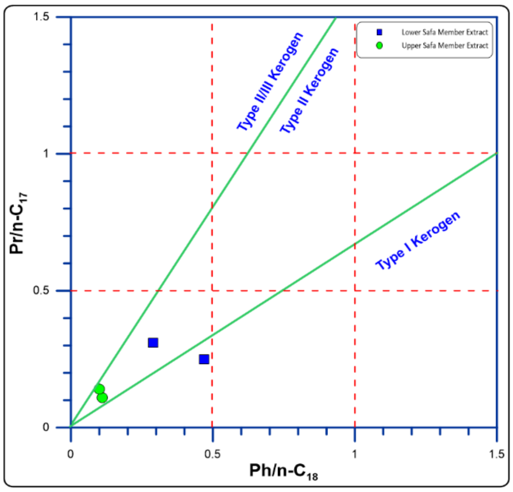

Fig. 14. Cross plot of Pr/n-C_{17} versus Ph/n-C_{18} for the analyzed samples (Obermajer et al., 1999).

References

Abdelbaset, m., Bosworth, b., Hammed, m. (2022). Structural evolution and petroleum system of the mesozoic faghur rift basin at the northwestern desert of egypt. Egyptian journal of geology, 2022; 66(1) pp. 83-96.

Abd El-Gawad, E.A., El Sheikh, A., Afify, W., Salem, T. (2015). Petroleum system evaluation of Jurassic and Paleozoic sections in Faghur Basin, Northwestern Desert. Egypt. Inter. J. Sci. Eng. App. Sci. 1 (9), pp. 387-407.

Abdullah, W. H. (1999). Organic facies variations in the Triassic shallow marine and deep marine shales of central Spitsbergen, Svalbard, Marine and Petroleum Geology, Volume 16, Issue 5, pp. 467-481.

Akinlua, A., Ajay, T.R. and Adeleke, B.B. (2007). Organic and inorganic geochemistry of northwestern Niger Delta oils. Geochemical Journal, V. 41, pp. 271-281.

Al-Sharhan, A.S., Abdel-Gawad, E.A. (2008). Geochemical characterization of potential Jurassic/Cretaceous source rocks in the Shushan Basin, northern Western Desert, Egypt. Journal of Petroleum Geology, V. 31, pp. 191-212.

Bosworth, William & Abrams, Michael & Drummond, Michael & Thompson, Melissa. (2015). Jurassic rift initiation source rock in the Western Desert, Egypt - relevance to exploration in other continental rift systems.

Carvajal-Ortiz, H., Gentzis, T. (2015). Critical considerations when assessing hydrocarbon plays using Rock-Eval pyrolysis and organic petrology data: Data quality revisited. International Journal of Coal Geology, V. 152, pp. 113-122.

Collister, J., Ehrlich, R., Mango, F., and Johnson, G. (2004). Modification of the petroleum system concepts: Origin of alkanes and isoprenoids in crude oils. AAPG Bull. V. 88, pp. 587-611.

Dahl, B., Bojesen-Koefoed, J., Holm, A., Justwan, H., Rasmussen, E. and Thomsen, E. (2004). A new approach to interpreting Rock-Eval S2 and TOC data for kerogen quality assessment. Organic Geochemistry, V. 35, pp. 1461-1477.

Daly, A., & Edman, J. (1987). Loss of organic carbon from source rocks during thermal maturation (abs.). AAPG Bulletin, 71, p. 546.

Deaf A.S. (2021). Sequence stratigraphy and distribution of organic-rich Lower Cretaceous mixed clastic-carbonate strata in Matruh Basin, northwestern Egypt: Constrains on the Tethyan sea level changes, palaeoclimate, and tectonics, Marine and Petroleum Geology, 129, 105105.

Didyk, B.M., Simoneit, B.R.T., Brassell, S.C. and Eglinton, G. (1978). Organic geochemical indicators of palaeoenvironmental conditions of sedimentation. Nature, V. 272, pp. 216-222.

Dolson, J. (2020). The petroleum Geology of Egypt and history of exploration. In: Hamimi, Z., et al. (Eds.), The Geology of Egypt. Regional Geology Reviews, pp. 636–658.

El Diasty, W.Sh. (2015). Khatatba Formation as an active source rock for hydrocarbons in the northeast Abu Gharadig Basin, northwestern Desert. Egypt. Arab. J. Geosci. 8 (4), pp. 1903-1920.

El Sharkawy, Y. (2018). New oil discoveries: boost Western Desert prospects. https://egyptoil-gas.com/features/new-oil-discoveries-boost-western-desert-prospects/. (Accessed 20 October 2020).

Espitalie, J., Laporte, L., Madec, M., Marquis, F., Leplat, P., Paulet, J. and Boutefeu, A. (1977). Methode rapid de caracterisation des rocks meres, de leur potential petrolier et leur degree devolution. Rev. Inst. Fr. Pet., 32 (1), pp. 23-42.

Espitalie, J., Deroo, G. and Marquis, F. (1985). “Rock-Eval pyrolysis and its application”. Inst. Fr. Pet. Preprint 33578, p. 72.

Felestteen, A.W., El-Soughier, M.I., Mohamed, M.S., Monged, M.N.S. (2014). Hydrocarbon source potential of the Jurassic sediments of Salam-3X borehole, Khalda Concession, Northwestern Desert, Egypt. Arab. J. Geosci. 7 (9), pp. 3467–3480.

Hunt, J.H. (1996). Petroleum geochemistry and geology. 2nd ed. Freeman and Company. New York, p. 743.

Jackson, K.S., Hawkins, P.J., and Bennett, A.J.R. (1985). Regional facies and geochemical evaluation of southern Denison Trough. APEA Journal, V. 20, pp. 143-158.

Khalda (2001). Khalda internal report after approving from EGPC. Egypt.

Langford, F.F. and Blank-Valleron, M.M. (1990). Interpretation of Rock-Eval pyrolysis data using pyrolyzable hydrocarbons vs. total organic carbon. AAPG Bulletin,V. 76, pp. 799-804.

Lijmbach, G. M. (1975). On the origin of petroleum. Proceedings of the 9th World Petroleum Congress, V. 2, pp. 357-369.

Michael A. Abrams, Matthias D. Greb, James W. Collister, Melissa Thompson (2016). Egypt far Western Desert basins petroleum charge system as defined by oil chemistry and unmixing analysis, Marine and Petroleum Geology, Volume 77, 2016, Pages 54-74.

Obermajer, M., Fowler, M.G. and Snowdon, L.R. (1999) Depositional environment and oil generation in Ordovician source rocks from southwestern Ontario, Canada: Organic geochemical and petrological approach. AAPG Bulletin, V. 83, pp.1426-1453.

Peters, K. E. and Cassa, M. R. (1994). Applied source rock geochemistry. the petroleum system-from source to trap (L. B. Magoon and W. G. Dows, eds.), AAPG, Tulsa, OK, pp. 93-117.

Peters, K.E., Fraser, T.H., Amris, W., Rustanto, B. and Hermanto, E. (1999). Geochemistry of crude oils from eastern Indonesia. AAPG Bulletin, V. 83, pp.1927-1942.

Philp, R.P. (1985). Fossil fuel biomarkers: Applications and Spectra. Elsevier, Amsterdam, p. 294.

Powell, T.G. and Mckirdy, D.M. (1973). Relationship between Ratio of Pristane to Phytane, Crude-Oil Composition and Geological Environment in Australia. Nature Physical Science, V. 243, pp. 37-39.

Shalaby, M.R., Hakimi, M.H., Abdullah, W.H. (2011). Geochemical characteristics and hydrocarbon generation modeling of the Jurassic source rocks in the Shoushan Basin, northwestern Desert, Egypt. Mar. Petrol. Geol. 28 (9), 1611–1624.

Shekarifard A., R Daryabandeh M., Rashidi M., Hajian M. and Röth J. (2019). Petroleum geochemical properties of the oil shales from the Early Cretaceous Garau Formation, Qalikuh locality, Zagros Mountains, Iran, International Journal of Coal Geology, V. 206, pp. 1-18.

Tissot, B., Durand, B., Espitalie, J. and Compaz, A. (1974). Influence of nature and diagenesis of organic matter in formation of petroleum, AAPG Bulletin 58, no. 3, pp. 499-506.

Williams, A., Kloster, A., Duckworth, R. and Piggott, N. (1995). The role of the Airborne Laser Fluorosensor (ALF) and other seepage detection methods in exploring frontier basins. In: Hansjien, S. (Ed.), Petroleum Exploration and Exploitation in Norway, NPF Special Publication, pp. 421-431.

تقييم صخر المصدر لوحدات صخور الجوراسي لحقل إمحوتب، حوض مطروح، الصحراء الغربية، مصر

على الشوربجي[١]، ودعاء موسي[٢]، ومحمود زين الدين[١]

[١] قسم الجيولوجيا، كلية العلوم، جامعة الأزهر ١ شارع المخيم الدائم، مدينة نصر، القاهرة، مصر

[٢] قسم الاستكشاف، معهد بحوث البترول المصري، مدينة نصر، القاهرة، مصر

تكشف المزيد من التقنيات المتقدمة في التقييم الجيوكيميائي العضوي وتكامل علوم الأرض عن مزيد من الفهم لحقول النفط. يمثل حقل إمحوتب أحد حقول النفط في الصحراء الغربية. تهتم الدراسة بعمل تقييم جيوكيميائي متكامل وتكوين صورة كاملة وواضحة عن النظام البترولي في الحقل. تم اختيار أربعة وثمانين (٨٤) عينة من الآبار و"٤" عينات مستخرجة تمثل عضوي الصفا السفلي والصفا العلوي من خمسة آبار (Imhotep-1X وImhotep-2X و Imhotep W-1X وImhotep S-1X وImhotep S- 3X) لإجراء هذه الدراسة. تم فحص العينات باستخدام تقنيات LECO C230 وRock-Eval-6 وGC. محتوى الكربون العضوي للوحدات الصخرية محل الدراسة يتراوح من فقيرة إلى ممتازة بالإضافة إلى احتمالية كونها مقبولة أو ممتازة بالنسبة للمحتوى البترولي. تم عمل تقييم للنضوج الحراري باستخدام درجة الحرارة القصوى ومعامل الفيترينيت (Ro)، والتي بينت أن العينات المدروسة تحتوي على نسب عالية من معامل المحتوى الهيدروجيني (HI)، والتي تعكس وجود عينات عالية النضوج ووصولها لمرحلة إنتاج الغاز، ويؤكد ذلك وجود كيروجين من النوع الثاني والثالث، الذي يتميز بإنتاج كلا من الزيت والغاز، وهذا يعكس القدرة على توليد الغاز والزيت والوصول إلى المرحلة النهائية من توليد الزيت. تشير نتائج GC إلى أن المادة العضوية ترسبت في بيئة بحرية – قارية وترسبت في بيئة مختزلة إلى شبه مؤكسدة.